We are IntechOpen, the world's leading publisher of Open Access books
Built by scientists, for scientists

4,800
Open access books available

122,000
International authors and editors

135M
Downloads

154
Countries delivered to

Our authors are among the

TOP 1%
most cited scientists

12.2%
Contributors from top 500 universities

CLARIVATE ANALYTICS
BOOK CITATION INDEX
INDEXED

WEB OF SCIENCE™

Selection of our books indexed in the Book Citation Index
in Web of Science™ Core Collection (BKCI)

Interested in publishing with us?
Contact book.department@intechopen.com

Thin Films for Immobilization of Complexes with Optical Properties

Joana Zaharieva and Maria Milanova

Additional information is available at the end of the chapter

Abstract

Thin film deposition techniques, such as dip coating, spin coating, and spray pyrolysis, are applied for the production of SiO_2-, poly-(methylmethacrylate) (PMMA)-, and SiO_2-/polyester-based "hybrid" matrices. The factors influencing the film properties are briefly discussed. The morphology of the films presented is studied by different microscopy techniques such as atomic force microscopy, electron (scanning and transmission) microscopy, and fluorescence microscopy. The composites based on SiO_2-, PMMA-, and SiO_2/polyster "hybrid" matrices possess the optical properties of the immobilized complexes of Ru(II) and Eu(III) with different organic ligands. The preparation of the PMMA matrix by the monomer methylmethacrylate polymerization (instead of using of PMMA solution) caused partial destruction of the less stable complexes and thereby a decrease in the fluorescence intensity.

Keywords: dip coating, spin coating, spray pyrolysis, SiO_2-based films, poly-(methylmethacrylate)-based films, SiO_2/polyester "hybrid" matrix, morphology, immobilization, composites, optical properties

1. Introduction

The methods applied for thin film production by deposition have been divided into two groups, physical and chemical, based on the nature of the deposition process [1]. Among them, the chemical methods include gas-phase deposition and solution techniques. The sol-gel process can produce glassy materials by reactions of precursors at room temperature. This process is suitable for thin film fabrication because the sol can easily be deposited on different substrates. It is very easily combined with deposition methods such as dip coating, spin coating, or spray pyrolysis. The convenience of such a combination will be shown in the chapter below along with the characterization of the films by different microscopy techniques such as

atomic force microscopy, AFM, and electron microscopy, transmission, TEM and scanning, SEM. The morphology of the sol-gel produced films coated on different substrates as well as their roughness, surface formations, and thickness are crucial parameters for the application of the films. One of the applications of such films is as a support matrix for the immobilization of complexes. The immobilization of complexes with optical properties in films and matrices is among the approaches applied to obtain new materials with interesting optical properties. Besides the fact that the new materials can possess the properties of both the complex and the matrix, the immobilization itself can improve the stability of the complex immobilized and can protect its properties, for instance, the quenching of fluorescence by the environment molecules. Three different types of composites with immobilized complexes were produced: SiO_2- and poly-(methylmethacrylate) (PMMA)-based composites as well as composites based on a SiO_2/polyester "hybrid" matrix. Complexes with different organic ligands of Ru(II) and Eu(III) were used because of their fluorescence in the visible region of the spectrum. The optical properties of the composites as well as the deposition techniques influencing them are presented.

2. Dip-coating technique

2.1. Advantages of dip-coating technique

Dip-coating is a low-cost, waste-free process that is easy to scale up and offers a good control on thickness of the films made by it, so it is popular in research and in industrial production as well. It has been demonstrated that the method is good enough to fill porosity, to make nanocomposites, as well as to perform nanocasting [2]. In spite of the ways of deposition proposed, involving a capillary induced convective coating [2], usually dip coating is combined with a sol-gel process and a substrate is immersed and withdrawn from a sol of the precursor at a certain rate, followed by evaporation of the solvent. Different substrates such as glass, polycarbonate and polymethylmethacrylate have been tested for production of transparent films of SiO_2, ZnO, indium tin oxide [3] as well as substrates such as Si, Si_3N_4 and SiO_2 for layers of γ-Fe_2O_3 nanoparticles [4].

The factors determining the structure of the films produced via dip coating such as structure of the precursors, relative rates of condensation and evaporation, capillary pressure, and substrate withdrawal speed are presented in [5–7]. An essential factor for the film quality is the film thickness, which is determined by the hydrolysis and condensation behavior characteristics of the precursors and depends on their concentration in the starting solution [8–12], the pH of the sol [13–15], the aging time [8, 12–14], the withdrawal speed [16, 17], the number of immersions, and the ratio of water and precursor [8, 13, 14, 16]. By careful control of hydrolysis and condensation reactions of selected precursors, various surface roughnesses and morphologies can be been achieved [18].

Information about the surface morphology including surface area and roughness is provided by an atomic force microscopy, AFM [18–20]. The united power of the SEM, TEM, and AFM methods contributes to the examination of the surface morphology of thin films prepared by the sol-gel technique using different types of precursors and different parameters of the dip-coating deposition procedure [19].

2.2. Films, matrices and composites produced by dip coating

2.2.1. Sol-gel produced SiO$_2$-based films and composites by dip coating

The process conditions as well as the solution properties are factors influencing the thickness and uniformity of thin films. The SiO$_2$-based films were made using Si-containing precursors such as the alkoxysilanes TEOS (tetraethoxysilane), OtEOS (octyltriethoxysilane), and MtEOS (methyl triethoxysilane). The latter two are also called organic modified silanes or ormosils because of the C-Si bond in the structure of these hybrid materials. On the surface, the silanol groups are replaced by alkyl groups that have a poor affinity for water so by that they are keeping the sol-gel surface hydrophobic [13]. Films deposited at a withdrawal speed of 0.4 mm/s with variations of the number of the immersions (from 1 to 7) on microscope glass using gels produced from TEOS, OtEOS, or mixtures of TEOS/OtEOS (mole ratio 1:1) as well as TEOS/MtEOS (mole ratio 1:3) were obtained, showing the influence of the alkoxysilane used [19]. It can be seen that the films obtained from pure TEOS sol have smooth, glassy surface (**Figure 1**). By using organic modified silanes (OtEOS, MtEOS), structuring of the surface is observed **(Figures 1–7),** and the appearance of formations with raindrop or ellipsoid shape with a widely varying size is observed; both the size and the concentration of the shapes depend on the film deposition conditions.
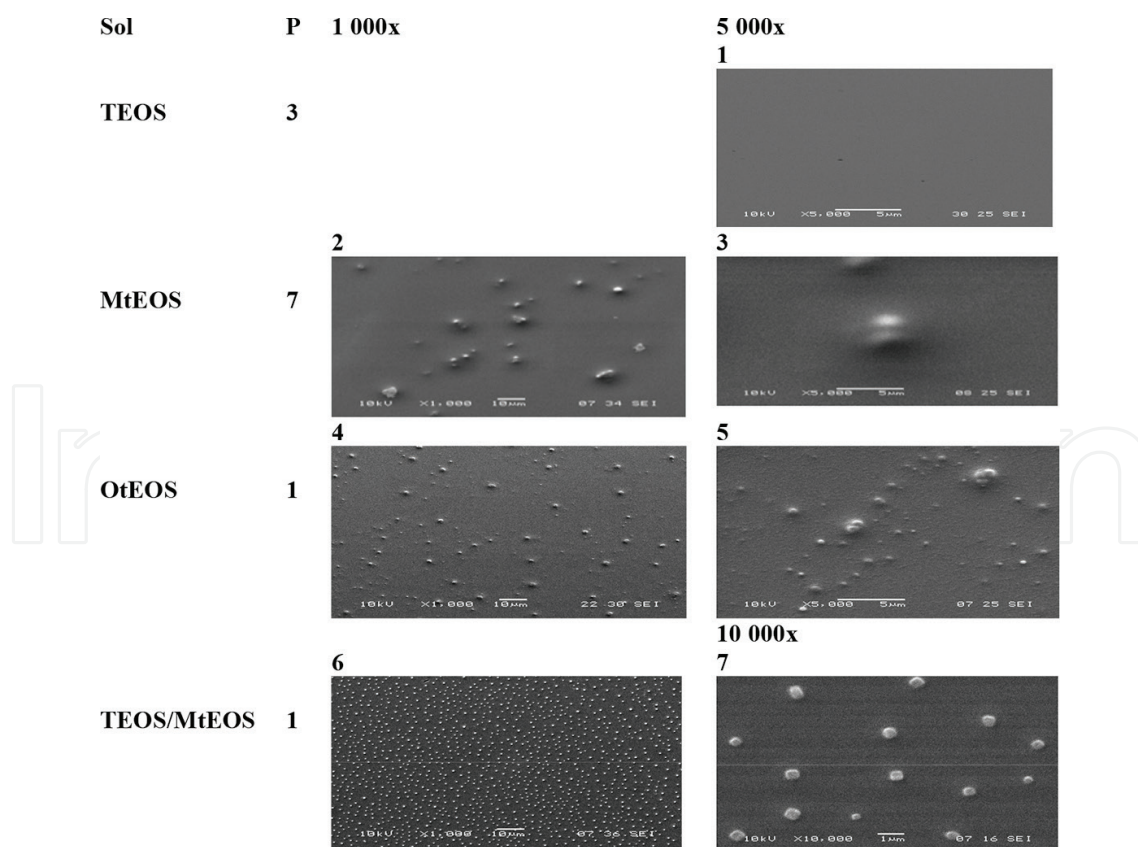

Figure 1. SEM images of films, obtained from different sols, at a withdrawing speed of 0.4 mm/s and different number of immersions, P [19].

SEM images of layers, prepared from TEOS, TEOS+MtEOS, MtEOS, and OtEOS containing sols with different numbers of immersions and different speeds (**Figure 2**), show the influence of these factors on the film morphology.
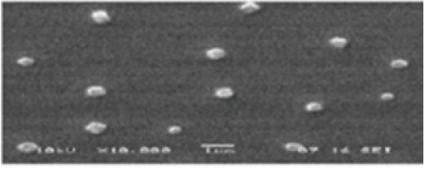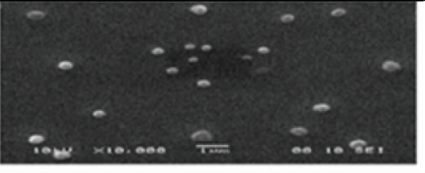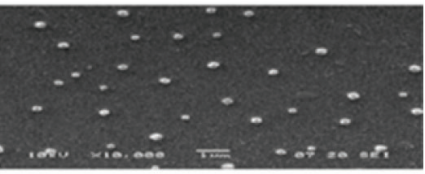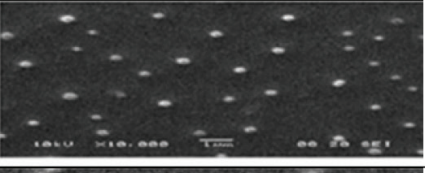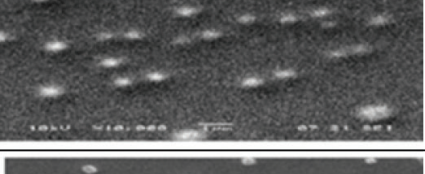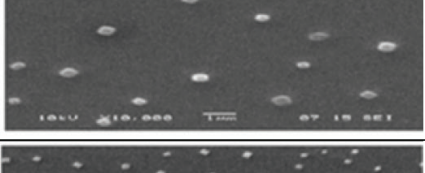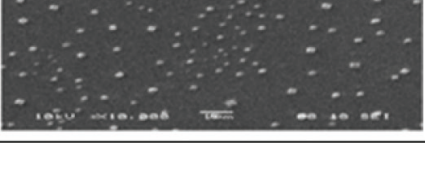
Films, 10 000 x	P	Dip speed, mm/s	Main grain size, nm
1	1	0.4	550 x 300
2	3	0.4	400 x 200
3	5	0.4	300 x 180
4	3	0.3	400 x 150 up to 1200 x 540
5	1	0.2	600 x 300
6	3	0.2	500 x 350
7	5	0.2	300 x 200

Figure 2. SEM images (10,000×) of the matrices, produced by dip coating from TEOS/MtEOS sol at different withdrawal speed and number of immersions, P [19].

The ellipsoid or rhombohedral grains observed (approximately 200 nm in size, **Figure 3**) showed a decreasing size and an increasing number per unit surface area with increasing number of immersions (**Figure 2**).
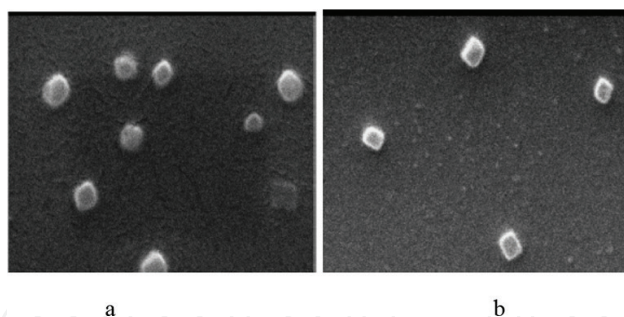
Figure 3. SEM image (30,000×) of the films obtained after (a) 3 and (b) 5 immersions with withdrawing speed (a) 0.3 and (b) 0.4 mm/s, produced from sol TEOS/MtEOS (ellipsoid or rhombohedral grains are approximately 200 nm in size) [19].

The dot distribution can be ascribed to and connected with the randomly formed macroscopic "pores" or hollows observed in the AFM images (**Figure 4**), with a higher concentration and better appearance in samples prepared with larger numbers of immersions.
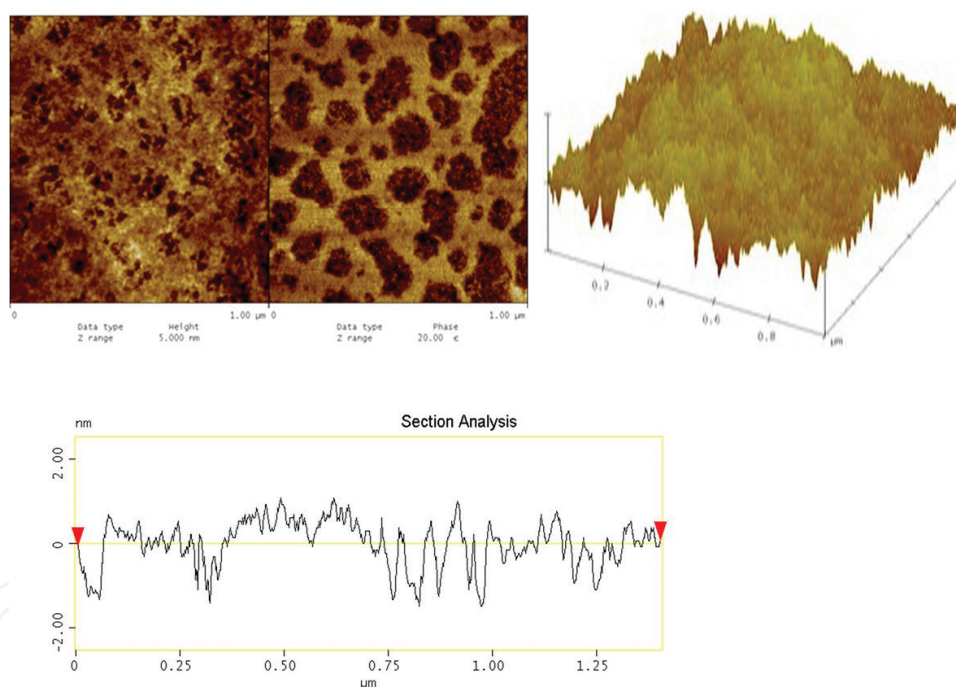

Figure 4. AFM images of films produced by dip coating (withdrawing speed 0.4 mm/s) from TEOS/OtEOS sol (1 immersion), bearing area 0.8 μm². The section analysis is performed along the diagonal of the bearing area [19].

Sol-gel produced SiO$_2$-based composites were made by orthosilanes with immobilization of the complex Rudpp, (Ru(II)-tris(4,7-diphenyl-1,10-phenanthroline) dichloride, [Ru(dpp)$_3$] Cl$_2$). The films produced (10–15 mm) from TEOS/OtEOS and Rudpp sols at withdrawal speed of 0.4 mm/s and up to 5 immersions have a good uniformity and thickness of about 500 nm. Smoothness of the films, combined with the good linkage between the layers, is ensured by these conditions [19]. The presence of Rudpp in the films produced from TEOS leads to the

appearance (due to microcrystallization of the Rudpp) of dots (**Figure 5b–d**) on the otherwise smooth surface of the Rudpp-free dip-produced film (**Figure 5a**).
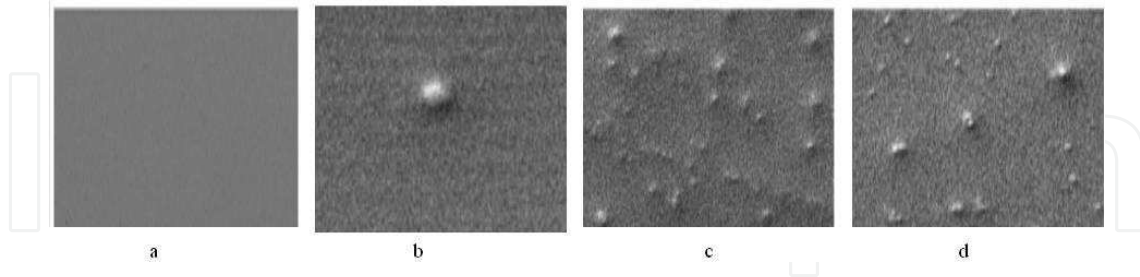

Figure 5. SEM images of layers without and with Ru(dpp), produced from TEOS-containing sols (a) TEOS (1), (b) TEOS-Rudpp (1), (c) TEOS-Rudpp (5), and (d) TEOS-Rudpp (7) (in brackets the number of the immersions) [19].

The synthetic conditions were improved by applying an ultrasound treatment to the sol after its magnetic stirring. It was found that this improves the surface of the films. Uniform, smooth films were obtained, and no microcrystallization of the complex was observed in the SEM or TEM images. Apparently, the ultrasound treatment of the sol is a powerful tool to avoid microcrystallization of the complex, leading to production of high-quality films. Films from non-sonicated sol show some heterogeneity due to micro-crystallization of the Rudpp [21] (**Figure 6**), whereas films produced from sonicated sol are entirely homogeneous [19].
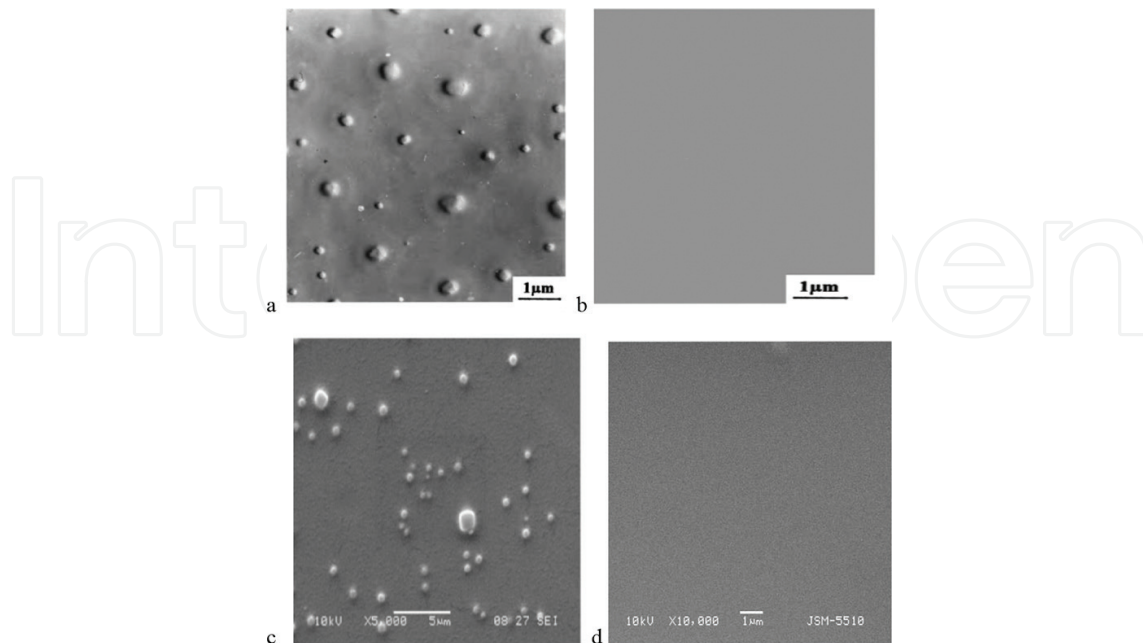

Figure 6. TEM (a, b) and SEM (c, d) images of TEOS/OtEOS/Rudpp dip-coated films without (a, c) and with (b, d) gel sonication [21].

The presence of OtEOS causes roughness of the films with sharply expressed hills and valleys as observed with AFM (**Figure 7b**). The chain-like surface structure in the OtEOS Rudpp film may be due to the presence of the long CH_3-$(CH_2)_7$ radicals that are likely difficult to fit into the SiO_2 network.
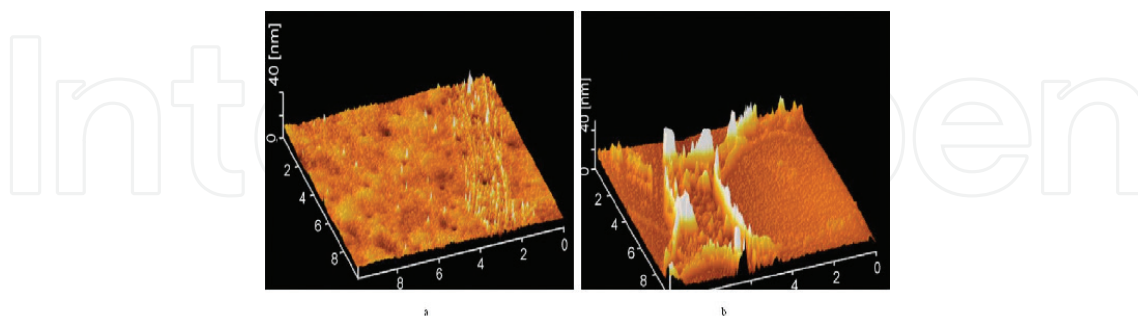

Figure 7. AFM images of films produced by dip coating (withdrawing speed 0.4 mm/s) from sols TEOS/OtEOS/Rudpp (a), and OtEOS-Rudpp (b); 1 immersion [19].

2.2.2. Sol-gel produced SiO_2-based matrix made from TEOS with immobilized $Eu(DBM)_3$ and $Eu(DBM)_3$·dpp complexes

A sol-gel produced SiO_2-based matrix was used for immobilization of the europium (III) complex with dibenzoylmethane (DBM), $Eu(DBM)_3$, and the mixed-ligand complex $Eu(DBM)_3$·dpp (dpp is 4,7-diphenyl-1,10-phenanthroline). The synthetic procedure for obtaining the composites is presented in [22]. To a magnetically stirred ethanol-dimethyl-formamide (DMF) solution (volume ratio 1:4) of the complex (2.5 g/dm^3), TEOS was added dropwise until an ethanol:TEOS mole ratio of 4 was obtained. After that water (with pH 8, adjusted by aqueous ammonia solution) was added in the same way, by this reaching mole ratio ethanol:TEOS:water = 4:1:4. Experiments with ratios 8:1:4 were also performed. After 2 h stirring, the sol obtained was aged at 50–70°C for different times. In some experiments, the fresh sol was sonicated for 30 min in an ice-water ultrasound bath. From the prepared gels, films with a typical thickness of ~300 nm were produced from one immersion with a with-drawing speed of 0.2 mm/s. Membranes (1–2 mm in thickness) were prepared by casting of a gel in a Teflon® mould. The influence of the temperature (ambient to 70°C) and time (3 h to 4 weeks) of ageing of the sol before film/membrane preparation and of their drying on the photoluminescence properties was investigated. When adding distilled water to the sol instead of water with pH = 8, a sol with pH of ~5 was obtained. Films produced from such sols showed no photoluminescence; it was concluded that the complex suffered destruction at this pH, by this the importance of pH control is shown [22]. Despite the positive effect of the sonication on the uniform distribution of the complex in the immobilization matrix [19], it caused quenching of the photoluminescence. This was probably due to some destruction of the complexes, and sonication is thus not recommended when these complexes are used. Emission spectra of the pure powdered complexes $Eu(DBM)_3$ and $Eu(DBM)_3$·dpp along with the SiO_2-based composites containing these complexes are shown in **Figure 8**. The charac-teristic emission band for Eu^{3+} is preserved in the spectra after immobilization.
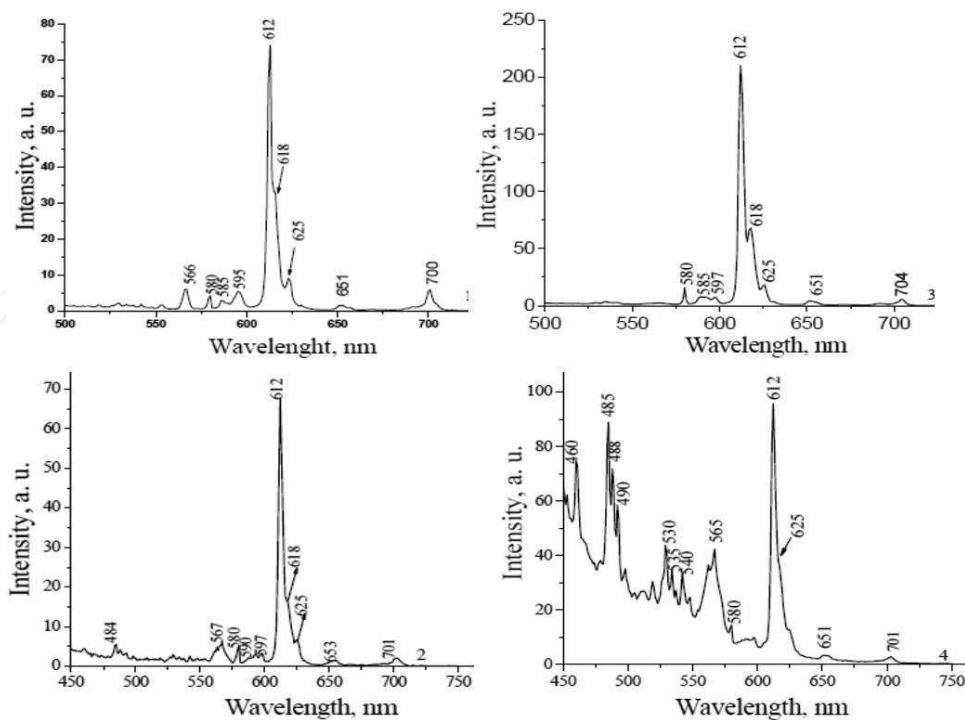
Figure 8. Emission spectra of Eu(DBM)$_3$ (1) and Eu(DBM)$_3$dpp (3) and of the composites containing Eu(DBM)$_3$ (2) and Eu(DBM)$_3$dpp (4) [22].

When larger amounts of DMF solvent were used than described above, it was found that after 6 weeks storage of the composites, they became opalescent and their optical properties changed. A possible explanation could be the disturbance of the Eu^{3+} coordination shell caused by the strong donor ability of the DMF. The presence of contaminant ions (using NaOH instead of NH$_4$OH for adjustment of the pH for alkoxide hydrolysis) strongly decreases the lifetime of the excitation states to 31 μs for Eu(DBM)$_3$ and to 19 μs for Eu(DBM)$_3$dpp containing composites, compared with 82 and 318 μs for the pure complexes, respectively.

2.2.3. SiO$_2$/polyester hybrid (inorganic/organic) matrix with immobilized Rudpp

Inorganic–organic hybrids combine the functional variety of organic compounds with the benefits of thermally stable and strong inorganic substrates and they can be promising precursors for immobilization matrices [23]. In the review quoted [23] different ways of making such "hybrid" materials are mentioned and among them is the simultaneous condensation of silica and organosilica precursors ("cocondensation"). A similar possibility is given by the application of the polymerized complex method [24], where a formation of polymeric resin is a result of condensation and polyesterification between a hydroxopolycarboxilic acid (preferably citric acid, CA) and a polyvalent alcohol (most often ethylene glycol, EG). If simultaneous hydrolysis of tetraethoxysilane (TEOS), esterification of the hydrolyzed product with CA, and esterification between CA and EG can happen, then it can be expected a formation more complicated structure in comparison with the relatively regular one obtained from pure TEOS. The formed polymer net may ensure suitable places for entrapping a complex and its uniform distribution (which may be very important, for example for gas sensor). Mole ratios

of TEOS:CA:EG = 4:1:1, 4:2:2, 2:1:1, and 1:1:1 were used, and an ultrasound treatment time was 40 min was applied. Substrates such as microscope glass were used. Before deposition, the slides were cleaned by 15 min treatment in an ultrasound bath consecutively with distilled water, methanol, acetone, and finally with distilled water. The factors influencing the properties of the composites synthesized based on SiO_2/polyester "hybrid" are (i) the mole ratio TEOS:CA:EG, (ii) the sol production method, (iii) the sol sonication, and (iv) the film thickness, determined itself by the sol composition, aging time, and withdrawing speed.

Microcrystallization of Rudpp complex was found to occur in a SiO_2 matrix produced from acid-catalyzed non-sonicated sol [21]; no indications for such a separation were found in the SiO_2/polyester "hybrid" films. Immobilization in the SiO_2/polyester films does not significantly change the fluorescent properties of the Rudpp complex, as shown in the fluorescence microscopy images (**Figure 9**).
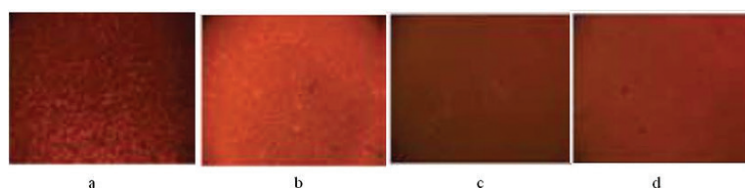
Figure 9. Images from fluorescence microscopy (×160) of films produced on microscope glass by dip coating at mole ratios TEOS:CA:EG = 4:1:1 (a), 4:2:2 (b), 2:1:1 (c), and 1:1:1 (d), respectively [25].

The fluorescence intensity from different regions of a "hybrid" film were followed in time. It can be seen that after a 150 s stabilization period, the fluorescence emission intensity from different regions stays constant within about 1.8% (**Figure 10**) [25].

Figure 10. Fluorescence intensity from different regions of a "hybrid" film as a function of time [25].

The matrix composition (ratio TEOS:CA:EG) does not influence the excitation (**Figure 11a**) and emission (**Figure 11b**) spectra of the films and the position of the maxima (310 and 619 nm, respectively).
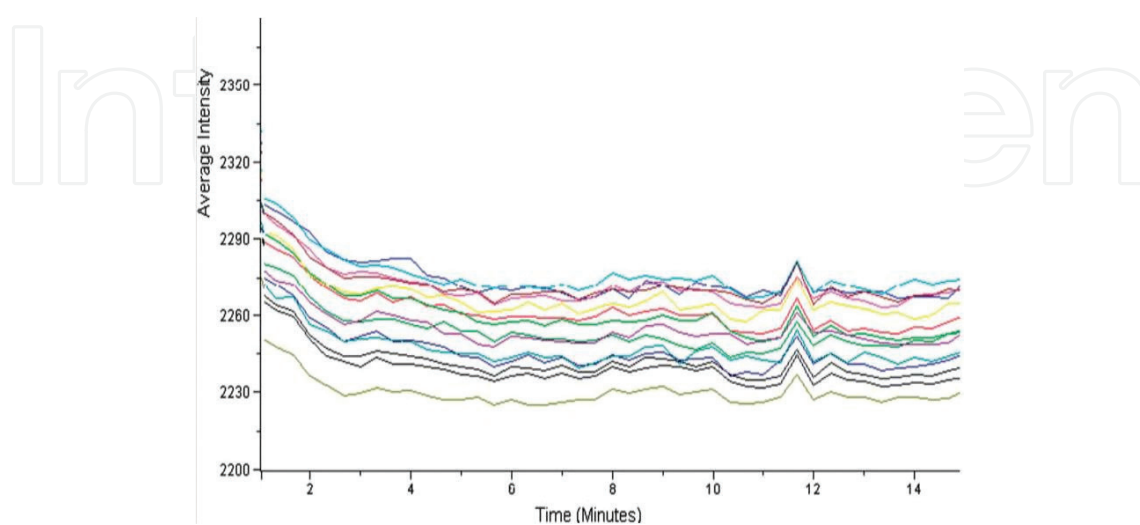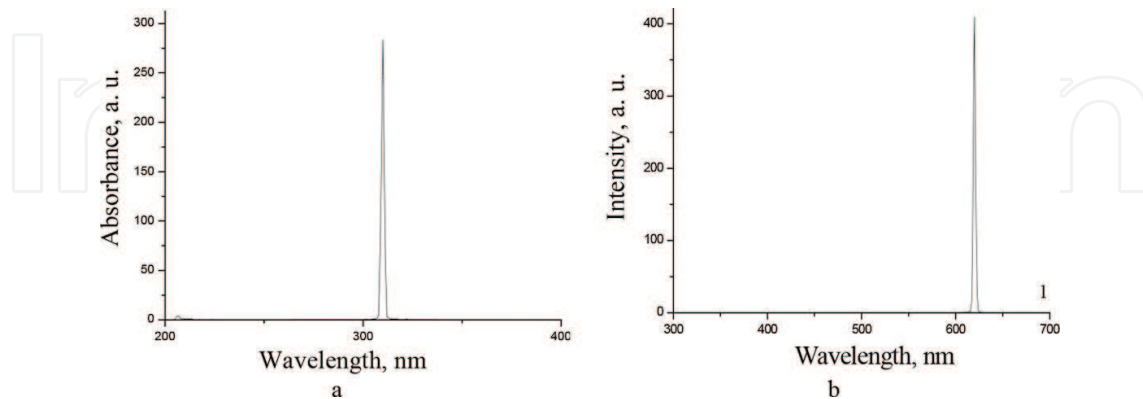

Figure 11. Excitation (a) and emission (b) spectra of Rudpp in hybrid matrix (TEOS:CA:EG = 4:1:1) [25].

The results obtained gives the opportunity to conclude that by formation of SiO_2/polyester "hybrid" matrix the films can be produced with a good stability, density and homogeneity, as well as with a good adhesion to different substrates such as glass, silica, and ceramics. An additional advantage of that matrix is the uniform distribution of the optically active complex immobilized, especially the fact that it preserves its optical properties. The film morphology strongly depends on the sol composition and deposition mode. Films prepared by dip coating at a withdrawing speed of 0.4 mm s^{-1} from sonicated sol with molar ratio TEOS:CA:EG = 4:1:1 produced by acid catalysed hydrolysis were found promising as an active component of optical sensors [25].

2.2.4. Composites based on poly-(methylmethacrylate), PMMA, with immobilized complexes

2.2.4.1. Immobilization of Rudpp in PMMA-based composites

A PMMA matrix was prepared by a catalytically induced polymerization of the monomer methylmethacrylate (MMA), following a procedure described in [26]. It was found that poly(methylmethacrylate) films produced from monomer, containing 1.5% Rudpp, are dense with a smooth surface and uniform distribution of the complex (**Figure 12a, b**) and fluorescent properties (**Figure 12c**). The fluorescence emission intensity from films produced by polymerization of the monomer MMA was significantly (2.5-fold) weaker in comparison with those prepared from PMMA solution, probably due to partial destruction of the complex.

Using a chloroform solution of PMMA, membranes and thin films of good quality can be obtained. Membranes (0.4–1.5 mm in thickness) were prepared by casting of the PMMA solution or partially polymerized MMA into a Teflon® mould. Both types of samples were dried at 50°C for 24 h. The use of PMMA as an immobilization matrix for Rudpp is a cheap and easy to be applied composite preparation method, ensuring the production of dense and smooth

specimens with uniformly distributed optically active complex with the possibility to prepare membranes up to 1 mm thick. No significant interaction of the complex with the matrices takes place, and the emission spectra of the complexes are practically unchanged as a result of immobilization in both types of studied matrices (**Figure 13a, b**). The reported results show the preparation of PMMA by the polymerization of the monomer MMA in the presence of benzoyl peroxide as a polymerization initiator is not a suitable method for the production of Rudpp-PMMA composites due to a partial destruction of the complex.
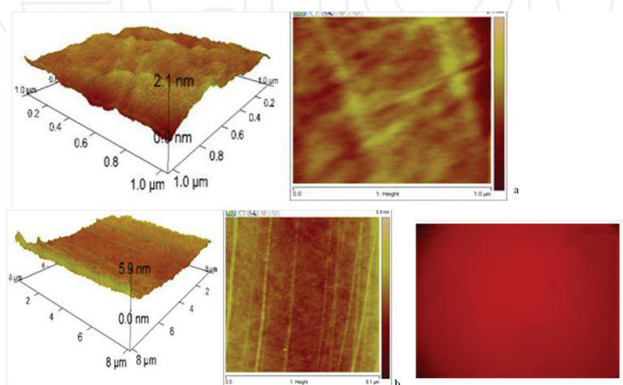

Figure 12. AFM (at different scanning area) (a, b) and fluorescence (x160) (c) images of dip-coated films from Rudpp-containing composite prepared from catalyst-induced polymerization of MMA [26].
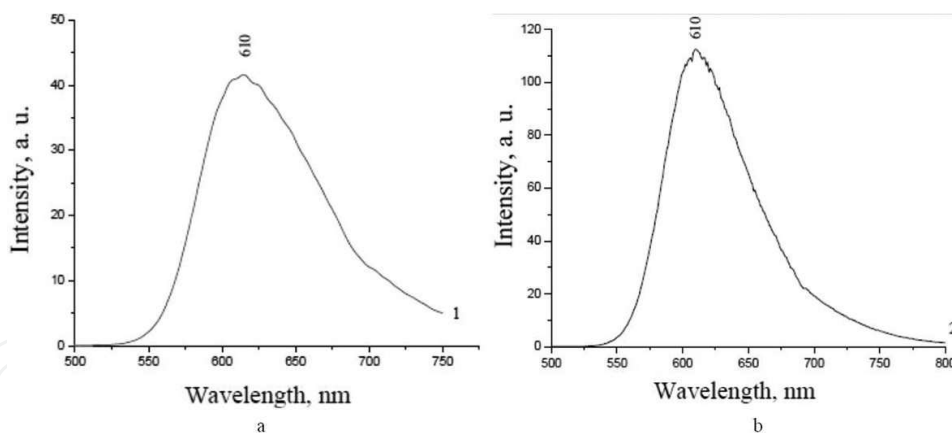
Figure 13. Emission spectra of a PMMA/Rudpp-containing membrane (excitation at 450 nm) prepared from catalyst-induced polymerization of MMA (a) and from PMMA solution (b) [26].

2.2.4.2. Immobilization of Eu(III) beta-diketonates in PMMA

The optically active complexes (Eu(DBM)$_3$, Eu(DBM)$_3$·phen, Eu(DBM)$_3$·dpp, Eu(TTA)$_3$·phen, and Eu(TTA)$_3$·dpp) are well-known fluorescent dyes with high fluorescent emission intensity (phen is phenanthroline, and TTA is thenoyltrifluoroacetone). The complexes of the type Eu(DBM)$_3$·Q (Q is phen or dpp) are of special interest due to their higher stability (compared to Eu(DBM)$_3$) and increased luminescence intensity [27].

A PMMA matrix was prepared by a catalytically induced polymerization of the monomer MMA [28]. The deposited films were aged at 50°C for 4–6 h. The experiments showed that thicker membranes can be prepared by applying 24 h of aging time at the temperature mentioned. The content of the complex in the final product after evaporation of the solvent was determined to be 1.5%. Using a solution of PMMA, films were deposited and membranes were prepared with a complex concentration in the final matrix of 1.0%. Films were deposited by dip coating at a withdrawal speed of 0.4 mm/s, using the device described in [29]. The films were uniform with a typical thickness of 200 nm. By varying the withdrawal speed, films with thickness of 0.1–1 μm were prepared. Membranes 0.1–1 mm in thickness can be easily obtained by placing the initial complex-binder mixture in a mould or by pouring along glass slides. SEM (**Figure 14**) or AFM (**Figure 15**) showed that no microcrystallization or aggregation (observed for example in [30], reaching 10 nm in size) of the complexes in the matrix took place and that cracks in films and membranes were absent. Qualitative tests with adhesive tape and brass edge showed that films thicker than 400–500 nm have poorer adhesion to the microscope glass.
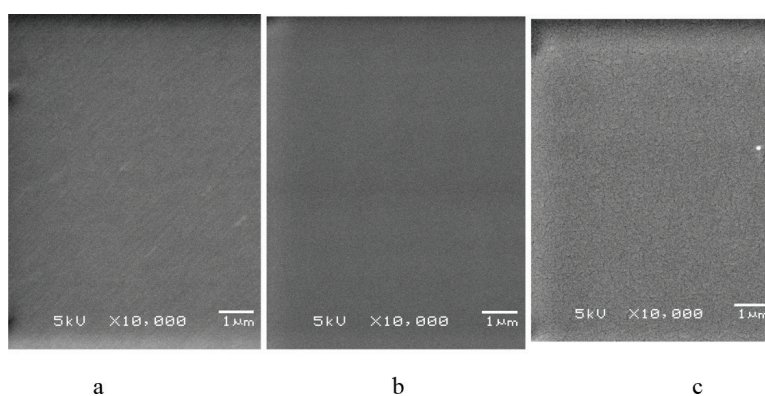
Figure 14. SEM images of dip -coated films of Eu(DBM)$_3$ (a) and Eu(TTA)$_3$phen (b, c,) in MMA (b) and PMMA (a, c) [28].
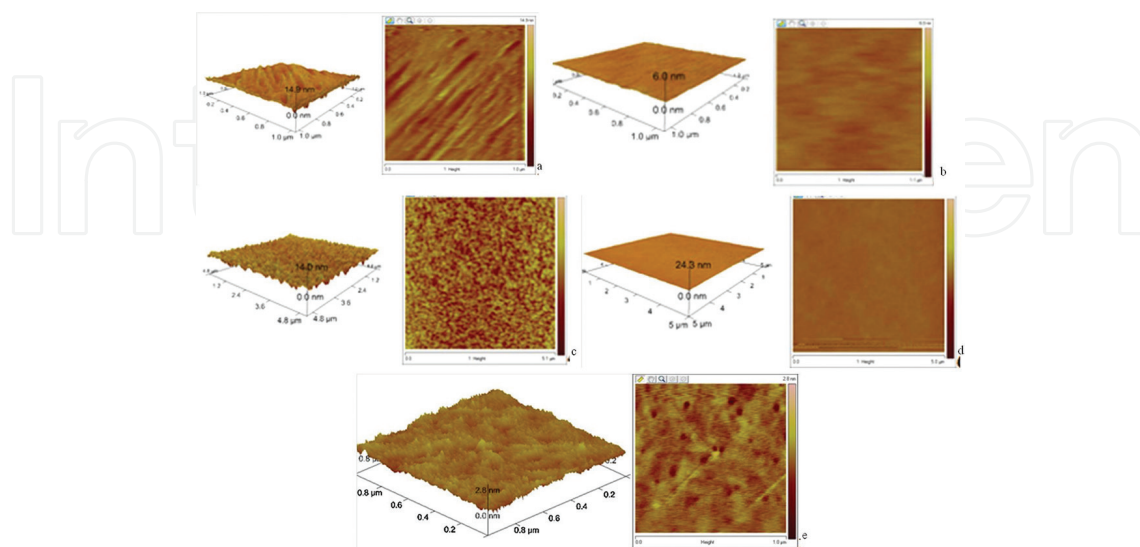
Figure 15. AFM images of dip-coated thin films of immobilized Eu complexes: Eu(DBM)$_3$ (a), Eu(DBM)$_3$phen (b), Eu(DBM)$_3$dpp (c), Eu(TTA)$_3$dpp (d) in PMMA, produced from the monomer, and Eu(DBM)$_3$ (e) in PMMA produced from polymer solution [28].

Embedding of the complexes causes some changes in the excitation spectra but does not influence the emission spectra significantly. The uniform distribution of the complex in the matrix and lack of aggregates, obtained by the applied deposition methods, also have a positive effect on the preservation of the lifetime of the excited states of the embedded complexes (**Figure 16**).
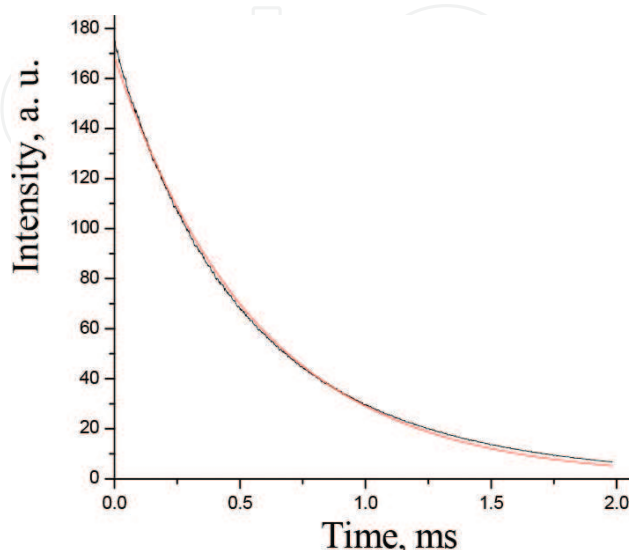

Figure 16. Lifetime of the excited state of composite Eu(TTA)$_3$phen in MMA [28].

The preparation of the matrix by the monomer polymerization leads to partial destruction of the less stable complexes and thereby a decrease in the fluorescence intensity. It was shown that the films produced by dip coating from europium-diketonates–PMMA chloroform solution can be used both as components of luminescent devices and for temperature sensing [28].

3. Spin-coating technique for film production

The basic principles of the spin-coating technique and the parameters controlling the process are presented, for example in Ref. [31], including the spin speed, spin time, acceleration, etc. The process generally involves four stages, namely a dispense stage (or deposition), substrate acceleration (spin-up) stage, a stage of substrate spinning at a constant rate, and evaporation [31, 32]. Evaporation may accompany the other stages [32, 33]. In order to understand the mechanism of thin-film formation by spin coating, the relationship between the thickness and the solvent evaporation rate of spin-coated thin films has been studied [34]. Spin coating combined with the sol-gel process offers a simple, low cost, and highly controlled way of film deposition [35]. In recent years, the method has been used for coating in microelectronics [36] and studied for deposition of transparent conducting oxides [37], for ferroelectric thin films [38], for indium oxide thin films [39], for doped and undoped hematite films [40], for ZnO thin films [35, 41–44], for titanium oxide films [45], for yttria-stabilized zirconia thin films [46], for mesoporous silica thin films on a silicon substrate [47], and so on.

3.1. SiO$_2$ films and composites produced by spin coating

The spin-coating technique was applied for sol-gel produced SiO$_2$-based films. The deposition was done by means of a KW-4A (USA) spin coater at 2000–6000 rpm, spinning time 20–60 s, and 1–3 spinning procedures (0.5 cm^3 sol per procedure) [19]. Different orthosilanes were used for SiO$_2$ precursors, such as TEOS, OtEOS, or their mixture. The morphology of the films prepared from TEOS and TEOS/OtEOS is shown in the SEM images (**Figure 17**).
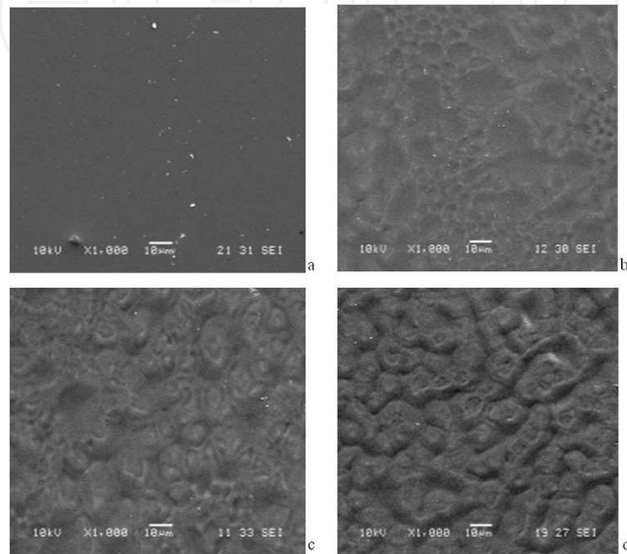

Figure 17. SEM images of films produced by spin coating at a spinning speed of 3000 min-1 from sols: TEOS (a); TEOS/OtEOS (b) (spinning time 30 s); TEOS/OtEOS (60 s), at an image angle of 90° (c) or 45°(d) [19].

The alkoxysilane used has an influence on the morphology of the spin-coated films. Films prepared using TEOS are similar to the dip-coated films (part 2.2.1.), that is, the films are dense and uniform (**Figure 17a**). The use of an ormosil-type precursor (TEOS/OtEOS mixture) leads to the production of "structured" films (**Figure 17b**) whose SEM images are different from those of dip-deposited films. The "structuring" improves with increasing of the spinning time from 30 to 60 s (**Figure 17b–d**), that is, with decreasing film thickness, which is opposite to the effect of the same parameter for dip coating.

A well expressed chain-like surface structure is seen in the AFM image (**Figure 18a**, without Rudpp) where the above mentioned hills and valleys are very regular. The section analysis (**Figure 18b**, with Rudpp) reveals hollows with diameters of 25–60 nm and depths of 1–1.6 nm and differences between the lowest and highest points in the scanned region of 2.8 nm. There is an influence of the spinning time: chains are observed at a spinning time of 60 s that are not noticed at 30 s spinning time (**Figure 17c, d**).

The thickness of the spin-produced films can be controlled by the gel spinning rate and the time. The thickness decreases with increasing spinning rate (2000–4000 min^{-1}) and time (20–40 s). The effect is significant (a factor two) when the spinning time was increased from
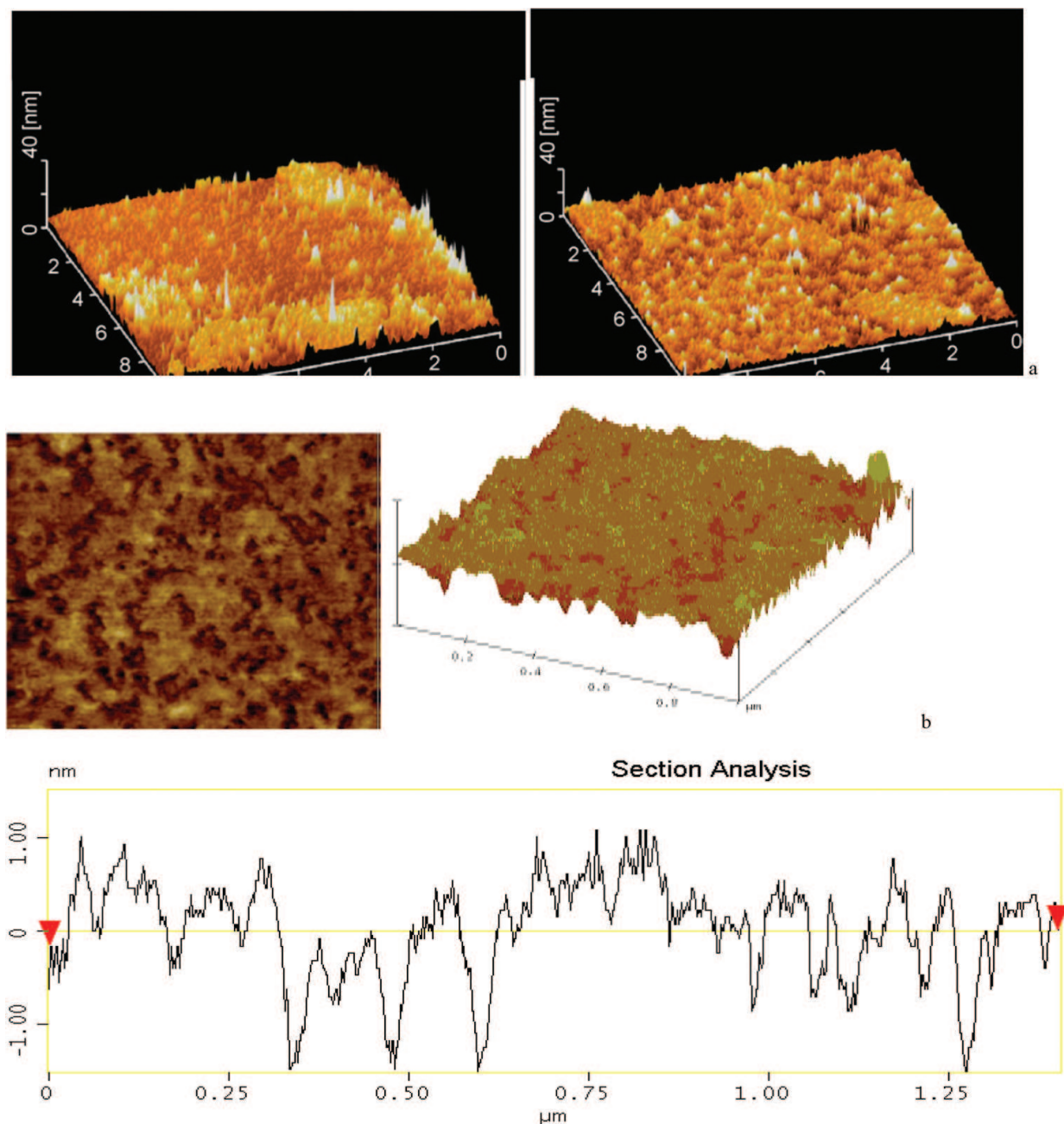
Figure 18. AFM images of films produced by spin coating (60 s, 3000 min⁻¹) from TEOS/OtEOS (a) and TEOS/OtEOS-Rudpp sol (b). The section analysis is performed along the diagonal of the bearing area [19].

20 to 30 s. No significant differences were found between films produced from TEOS/OtEOS and pure TEOS at spinning times of 30 and 40 s [21]. The thickness of the produced films (1 × 1 cm), measured by a Talystep profilomer, depends on the deposition conditions and is typically around 300 nm for dip-coated films. The thickness of the spin-deposited films is much larger: from 7 μm (at 0.5 cm^3 gel, 3000 rpm, 30 s) to 19 μm (1.5 cm^3 gel, 2000 rpm, 20 s) [19]. Their morphology depends mainly on the nature of the precursor and somewhat on the deposition method [19].

The ruthenium complex Rudpp was immobilized in a SiO_2 matrix by following a commonly used sol preparation procedure (with 1.25–2.5 g Rudpp/dm^3 sol). It was found that microcrystallization of the complex occurs with formation of randomly distributed crystals of 100–400 nm in size. An ultrasound treatment of the sol by means of an ultrasound disintegrator leads to homogeneous distribution of the complex without observable crystallization (**Figure 18b**).

3.2. Rudpp complex immobilized in a SiO_2/polyester "hybrid" composite

A SiO_2/polyester "hybrid" with immobilized Rudpp complex was prepared, using a polished fused silica substrate spinning at 2000 min^{-1} and a precursor solution with mole ratio TEOS:CA:EG = 1:2:2. The sol aging time was 2 h, the spraying/spinning time was 30 s, and ultrasound treatment time was 40 min [21]. It was found that the spin-produced specimens obtained from sols enriched in CA and EG were not uniform.

4. Spray pyrolysis method for film production

Spray pyrolysis is a simple and inexpensive technique, which does not require high-quality substrates or chemicals for the production of various materials. It is easy for preparing films of any composition, such as thin films with large surface area, ceramic coatings, dense films, porous films at relatively low temperatures, and multilayered films [1].

It has been used for decades in the glass industry and in solar cell production [1], for powder production [48] and for electrodes and counter electrodes for dye-sensitized solar cells [49]. The method is used for deposition of thin ferrite films [50], thin films of the perovskite $LaFeO_3$ [51], thin films of TiO_2 (pure or modified) [52–55], films of poly-(methyl)methacrylate [28], and thin films of cerium-doped yttrium-iron garnet [56], each of them with potential applications in water purification, oxygen sensing, thermosensors, for deposition of thin yttria-stabilized zirconia films [1, 57, 58], for crystalline and non-crystalline iron oxide (α-Fe_2O_3) thin films onto glass substrates at different temperatures [59, 60], highly structured ZnO layers [61], transparent conducting zinc oxide thin films [62], lead(II) oxide thin films [63], nanoporous aluminum oxide [64], europium doped lanthanum oxide films [65], and UV excited green emitting Eu(II) activated $BaAl_2O_4$ and $SrAl_2O_4$ [66] and etc. Typical spray pyrolysis equipment consists of an atomizer, precursor solution, substrate heater, and temperature controller. The atomizers usually used in spray pyrolysis technique are mentioned and explained in [1], namely air blast (the liquid is exposed to a stream of air), ultrasonic (ultrasonic frequencies produce the short wavelengths necessary for fine atomization), and electrostatic atomizer (the liquid is exposed to a high electric field).

4.1. Factors influencing the properties of the films produced by spray pyrolysis

The processes involved in the spray pyrolysis technique as well as the effects of spray pyrolysis parameters on film quality such as the influence of the substrate surface temperature on the film roughness, cracking, and crystallinity are discussed in Ref. [1]. The substrate surface temperature is a parameter that determines the film morphology and properties so that by increasing the temperature, the film morphology can be changed from a cracked to a porous microstructure [1]. The influence of different parameters on the thickness, morphology, crystal

structure, and adhesion of the films is discussed in [5, 67], and optimal values are given (in brackets) for the nature of the carrier gas (oxygen or nitrogen) and its flow rate (0.5–1.2 dm^3/min), the substrate temperature during the spraying (350°C or 400°C), the spraying angle (varied in the interval 20°–90°), the distance between the substrate and the nozzle (15–25 cm), the duration of spraying (10–20 s), the interval between the consecutive sprayings (1–5 min), the number of sprayings (1–20 cycles), the postdeposition annealing temperature (350–480°C), and the type of substrate. A comprehensive model for spray pyrolysis using solutions is presented in [67]. Different solutions or suspensions have been used such as ethylene glycol solution of mixed metal citrate complexes [67, 68] and aqueous or methanol suspensions containing TiO$_2$ and EG or PEG [54]. In some of the experiments, sonication for 20 min by means of ultrasonic disintegrator, UD, 20 (Technopan, Poland) was applied before spraying [54]. The device used [69] is suitable for film deposition. The suspension was passed through a pneumatic nebulizer with a 1 mm nozzle diameter using pressurized O$_2$ [5, 54] or N$_2$ [50] as a carrier gas. A nebulizer with nozzle of 0.7 mm in diameter was also used [50]. Microscope slides and optical grade glass of various shapes and sizes were used [51]. The substrate was situated at 20 cm from the nozzle at an angle of 45° and heated at temperatures, depending on the nature of the substrate and of the spraying material and kept within the limits of ±5°C. The suspension was sprayed for 30 s periods, separated by intervals of 5 min. The deposited films were heated at 300–500°C for 1 h [54] or 480–750°C for 0.5–3 h [50] in static air. The prepared films had a very good adhesion to the substrate as demonstrated by the standard tests with scotch tape and brass edge. The film thickness was controlled by the number of spraying cycles [50]. Typically, 10 cycles can be applied to produce 0.5 mg/cm^2 layers of TiO$_2$ that were approximately 1.5 μm thick [54]. With O$_2$ as a carrier gas, more uniform films were formed compared with those prepared using N$_2$ at the same conditions. This is probably due to a more even and complete burning of the organic components in the initial solution, when citric complexes were applied as precursors (**Figure 19**) [51].
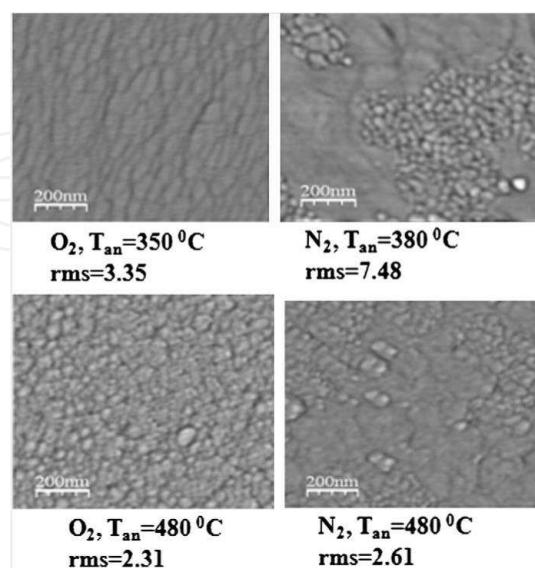

Figure 19. AFM images of films deposited on microscope glass slides at a substrate temperature of 350°C; as carrier gas are used O$_2$ or N$_2$, at a flow rate of 1 dm^3/min; annealing of the films in air for 3 h at 350°C (O$_2$-produced films) or 380°C (N$_2$-produced films) and at 480°C (rms: root mean square roughness) [51].

The method is suitable for the production of films up to ~700 nm thickness. The film thickness above 700 nm can cause cracking during the thermal treatment, following the deposition [51]. Thin films of $La_2Ti_2O_7$ were deposited by spray pyrolysis using as starting material the ethylene glycol solutions of La–Ti citric . The films produced on silica glass and Si substrates after 2 h postdeposition annealing at 750°C were with good stoichimetry, homogeneous and with highly crystallinity. It was found that the size of the crystallites was between 25 and 45 nm and it depended on the nature of the substrate and slightly on the conditions for deposition and postdeposition. Using the number of the spraying cycles, the thickness of the films can be controlled (up to 1.2 mm). The size of the grains may also be controlled by the diluents used and by the conditions for annealing [68]. Highly crystalline uniform Y_2O_3 films (0.2 1 μm) were obtained using EG solutions of yttrium citric complexes, demonstrating that thin films can be deposited using spray pyrolysis of nonaqueous solutions of citric complexes as a starting material and using O_2 as a carrier gas. The substrate was heated at 350°C during the deposition, and a postdeposition annealing at 850°C for 2 h was applied [70].

The optimal coating conditions were similar to the ones used in [53]. The suspension was passed through a pneumatic nebulizer with a 1 mm nozzle diameter using pressurized O_2 as a carrier gas. The substrate was situated 20 cm from the nozzle at an angle of 45° and heated at temperatures that depended on the nature of the substrate and of the spraying material. The suspension was sprayed for 30 s periods, separated by intervals of 5 min. The deposited films were heated at 300–500°C for 1 h in static air. The prepared films had a very good adhesion to the substrate as demonstrated by the standard tests with scotch tape and brass edge. The film thickness was controlled by the number of spraying cycles. Typically, 10 cycles can be applied to produce 0.5 mg/cm^2 layers that were approximately 1.5 μm thick [54].

4.2. Spray pyrolysis for immobilization of complexes and synthesis of composites with optical properties

4.2.1. PMMA-based composites

The composite $Eu(DBM)_3$/PMMA was obtained by two methods. The first one includes the dissolving of the complex into the MMA monomer solution followed by polymerization, and the second one includes the dissolving of the polymer and the complex in a solvent, followed by the evaporation of the latter. After the solution was prepared, the spray pyrolysis device, described in details in Ref. [69], was applied. The spraying conditions for $Eu(DBM)_3$-containing solution of MMA are as follows: a nebulizer with a nozzle diameter of 0.8 mm, under an angle of 45° and at a distance of 20 cm from the substrate surface was used. As a carrier gas, air was applied with a flow rate of 0.7–0.9 dm^3/min. The substrates used were heated at temperature varied between 50 and 70°C. The spraying time was 15 s, and the interval between different layer depositions was about 30 min. [28]. An example of the morphology of the films can be seen in **Figure 20**.

A tendency for decreasing film roughness when the monomer MMA polymerization was applied can be seen. This is explained by the relatively fast polymerization inside the very

small droplets as well as by the sharp temperature decrease in the solution containing oligo-merized monomer during deposition. This limits the possibility of formation of long chains and disturbs the structure obtained when PMMA polymer solution is used.
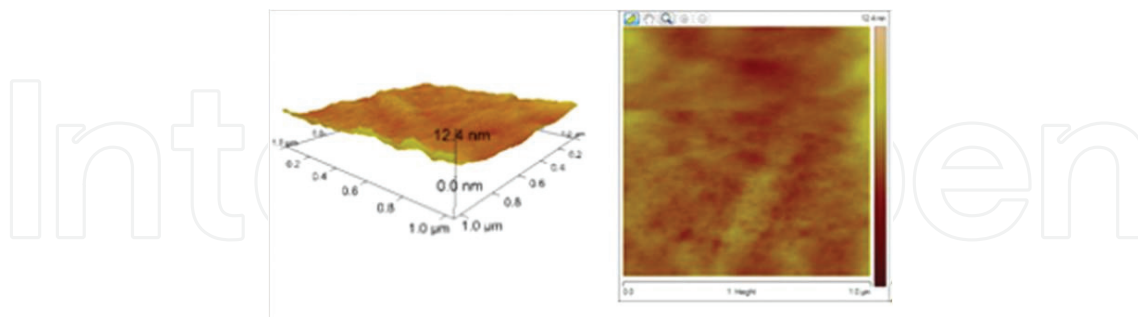
Figure 20. AFM-image of Eu(DBM)$_3$/PMMA film produced by spray coating [28].

The optical properties of the Eu(DBM)$_3$ complex and its derivatives as well as of Eu(TTA)$_3$·phen after their immobilization both in films and in membranes produced from MMA or PMMA solutions were followed. For both types of matrices, the excitation spectra of the complexes showed some changes (with general pattern preserved), whereas the emission spectra were not disturbed (**Figure 21**) [28].

Figure 21. Emission spectra of (a) complex in solid state, (b) immobilized in a matrix from MMA solution, and (c) immobilized in a matrix from PMMA solution [28].

The lifetime is 75, 214, and 265 μs for the pure Eu(DBM)$_3$ and the complex immobilized in MMA and in PMMA, respectively. The preparation of the matrix by monomer polymerization leads to partial destruction of the less stable complexes and thereby a decrease in the fluorescence intensity.
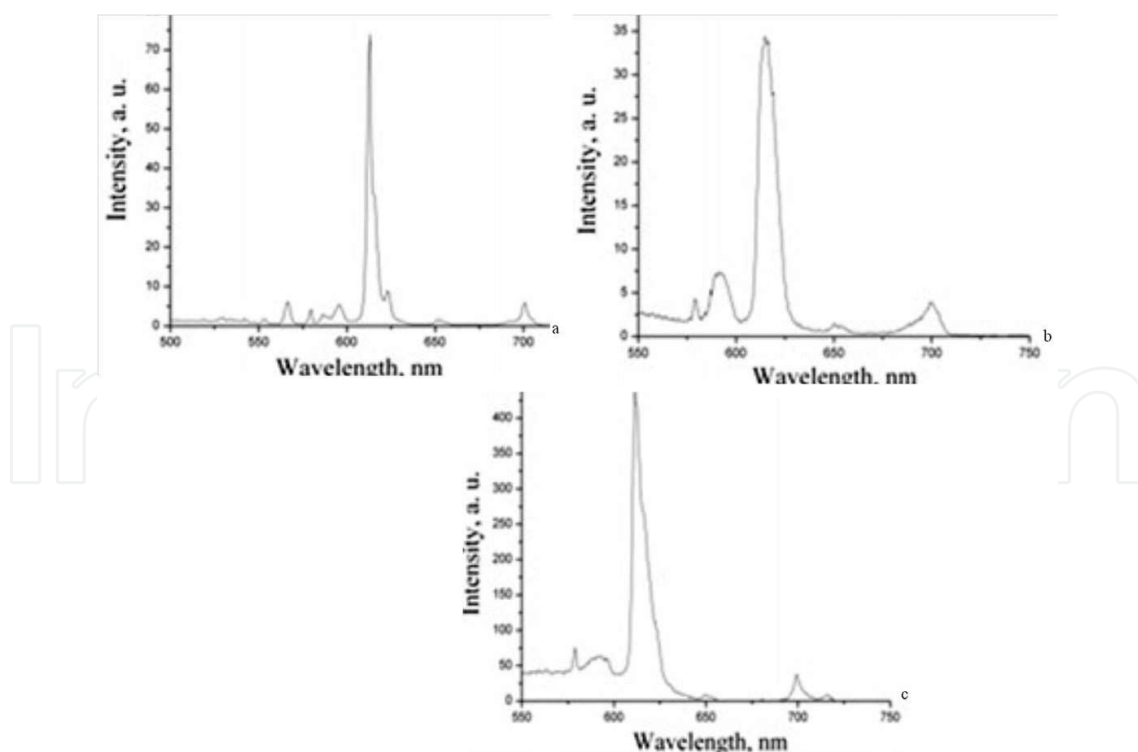
4.2.2. Spray pyrolysis produced composites based on SiO$_2$/polyester "hybrid" matrix

The synthetic procedure for composited preparation consists of citric acid (a measured amount) dissolved in ethanol under stirring, and of EG added in small portions to the solution obtained. Stirring for 15 min was applied in order to obtain a homogeneous final solution. To the latter one, TEOS was added dropwise in an amount that the desired mole ratio of TEOS:CA:EG:EtOH to be reached. By adding HCl (0.1 M), the pH value was adjusted equal to 2. To obtain a complex concentration of 2.5 g dm^{-3} sol, an ethanol solution of Rudpp (0.014 g mL^{-1}) was added. The variation of the complex concentration was experimented, but it did not show an effect on the main functional parameters of the films produced. The films produced by spray pyrolysis were uniform, without cracks and with a satisfactory adhesion, and contained pores that were about 100 nm in diameter (**Figure 22**).
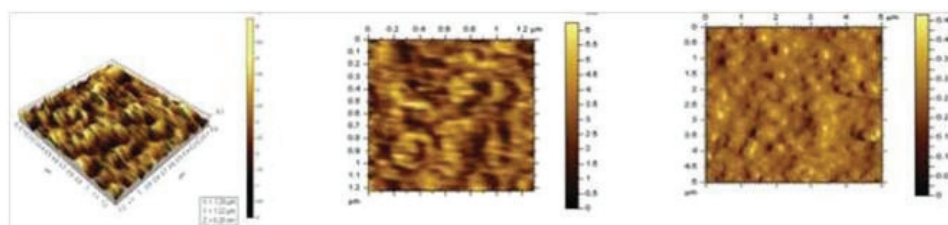
Figure 22. AFM images of based on SiO$_2$ polyester hybrid film made by spray pyrolysis [25].

The pores are probably due to the faster evaporation of the excess of EG in the course of spraying on the heated surface. It is concluded that the chain structure is common for spray-produced films based on SiO$_2$/polyester "hybrid" [25].

Author details

Joana Zaharieva* and Maria Milanova

*Address all correspondence to: jzaharieva@abv.bg

University of Sofia "St. Kliment Ohridski," Faculty of Chemistry and Pharmacy, Department of Inorganic Chemistry, Sofia, Bulgaria

References

[1] Perednis D, Gauckler LJ. Thin film deposition using spray pyrolysis. J Electroceram. 2005;**14**:103–111.

[2] Grosso D. How to exploit the full potential of the dip-coating process to better control film formation. J Mater Chem. 2011;**21**:17033-17038. doi: 10.1039/C1JM12837J

[3] Ebert D, Bhushan B. Transparent, superhydrophobic, and wear-resistant coatings on glass and polymer substrates using SiO_2, ZnO, and ITO nanoparticles. Langmuir. 2012;**28:**11391–11399. doi: 10.1021/la301479c

[4] Yoon T-S, Oh J, Park S-H, Kim V, Jung BG, Min S-H, Park J, Hyeon T, Kim K-B. Single and multiple-step dip-coating of colloidal maghemite nanoparticles onto Si, Si_3N_4, and SiO_2 substrates. Advanced Functional Materials, 2004;**14**:1062-1068.

[5] Todorovsky D, Todorovska R, Petrova N, Uzunova-Bujnova M, Milanova M, Anastasova S, Kashchieva E, Groudeva-Zotova S. Spray-pyrolysis and deep- or spin-coating deposition of thin films and their characterization. J Univ Chem Technol Metallurgy. 2006;**41**:93–96.

[6] Brinker CJ, Frye GC, Hurd AJ, Ashley CS. Fundamentals of sol-gel dip coating. Thin Solid Films. 1991;**201**(1):97–108. doi:10.1016/0040-6090(91)90158-T

[7] Brinker CJ, Hurd AJ. Fundamentals of sol-gel dip-coating. J Phys III. 1994;**4**:1231–1242. doi:10.1051/jp3:1994198

[8] MacCraith B, McDonagh C. Enhanced fluorescence sensing using sol-gel materials. J Fluorescence. 2002;**12**:333–342. doi:10.1023/A:1021301723885

[9] McDonagh C, MacCraith BD, McEvoy AK. Tailoring of sol–gel films for optical sensing of oxygen in gas and aqueous phase. Analyt Chem. 1998;**70**:45–50. doi:10.1021/ac970461b

[10] Ahmad M, Mohammad N, Abdullah J. Sensing material for oxygen gas prepared by doping sol–gel film with tris (2,2-bipyridyl)dichlororuthenium complex. J Non-Cryst Solids. 2001;**290**:86–91. doi:10.1016/S0022-3093(01)00719-0

[11] Mills A, Williams F. Chemical influences on the luminescence of ruthenium diimine complexes and its response to oxygen. Thin Solid Films. 1997;**306**:163–170. doi:10.1016/ S0040-6090(97)00246-0

[12] Lobnik A, Wolfbeis OJ. Probing the polarity of sol-gels and ormosils via the absorption of nile red. Sol–Gel Sci Technol. 2001;**20**:303–311. doi:10.1023/A:1008734320809

[13] McDonagh C, Bowe P, Mongey K, MacCraith BD. Characterisation of porosity and sensor response times of sol–gel-derived thin films for oxygen sensor applications. J Non-Cryst Solids. 2002;**306**:138–148. doi:10.1016/S0022-3093(02)01154-7

[14] McDonagh C, Shields AM, McEvoy AK, MacCraith BD, Gouin JF. Optical sol-gel-based dissolved oxygen sensor: progress towards a commercial instrument. J Sol–Gel Sci Technol. 1998;**13**:207–211. doi:10.1023/A:1008608901645

[15] McEvoy AK, McDonagh CM, MacCraith BD. Dissolved oxygen sensor based on fluorescence quenching of oxygen-sensitive ruthenium complexes immobilized in sol–gel-derived porous silica coatings. Analyst. 1996;**121**:785–788. doi:10.1039/AN9962100785

[16] McDonagh C, Sheridan F, Butler T, MacCraith BD. Characterisation of sol-gel-derived silica films. J Non-Cryst Solids. 1996;**194**:72–77. doi:10.1016/0022-3093(95)00488-2

[17] Tang Y, Tehan EC, Tao Z, Bright FV. Sol–gel-derived sensor materials that yield linear calibration plots, high sensitivity, and long-term stability. Analyt Chem. 2003;**75**:2407–2413. doi:10.1021/ac030087h

[18] Shang HM, Wang Y, Limmer SJ, Chou TP, Takahashi K, Cao GZ. Optically transparent superhydrophobic silica-based films. Thin Solid Films. 2005;**472**:37–43. doi:10.1016/j.tsf.2004.06.087

[19] Anastasova S, Milanova M, Kashchieva E, Funakubo H, Kamo T, Grozev N, Stefanov P, Todorovsky D. Morphology of sol-gel produced composite films for optical oxygen sensors. Appl Surf Sci. 2008;**254**:1545–1558. doi:10.1016/j.apsusc.2007.07.090

[20] Preininger C, Ludwig M, Mohr GJ. Effect of the sol-gel matrix on the performance of ammonia fluorosensors based on energy transfer. J Fluorescence. 1998;**8**:199–205. doi:10.1023/A:1022549531746

[21] Anastasova S, Milanova M, Rangelov S, Todorovsky D. Influence of the precursor nature and deposition mode on the oxygen sensing properties of Ru(II) complex immobilized in SiO_2-based matrix. J Non-Cryst Solids. 2008;**354**:4909–4916.DOI: 10.1016/j.jnoncrysol.2008.07.006

[22] Zaharieva J, Milanova M, Todorovsky D. Europium dibenzoylmethane complexes in SiO_2-based matrix. J Optoelectron Adv Mater. 2010;**12**:1247–1254.

[23] Hoffmann F, Cornelius M, Morell J, Froba M. Silica-based mesoporous organic–inorganic "hybrid" materials. Angew. Chem. Int. Ed. 2006;**45**:3216–3251

[24] Todorovsky DS, Getsova MM, Milanova MM, Kakihana M, Petrova NL, Arnaudov MG, Enchev VG. The chemistry of the processes involved in the production of lanthanide titanates by the polymerized complex method. Can J Chem. 2007;**85**:547–559. DOI: 10.1139/v07-067

[25] Zaharieva J, Milanova M, Todorovsky D. SiO2/polyester hybrid for immobilization of Ru(II) complex as optical gas-phase oxygen sensor. J Mater Chem. 2011;**21**:4893–4903. doi:10.1039/C0JM03169K

[26] Zaharieva J, Milanova M, Todorovsky D. Poly(methylmethacrylate) as immobilization matrix for Ru(II)-complex, a potential optical oxygen sensor. J Optoelectron Adv Mater. 2011;**13**:727–732.

[27] Zaharieva J, Milanova M, Todorovsky D. Synthesis conditions impact on the composition, structure, and fluorescence properties of the europium dibenzoylmethane complexes. Synth React Inorg Met Org Nano Met Chem. 2010;**40**:651–661.

[28] Zaharieva J, Milanova M, Todorovsky D. Poly-(methylmethacrylate) as immobilization matrix for europium-diketonates. Morphology and fluorescent properties. Appl Surf Sci. 2011;**257**:6858–6866.

[29] Dushkin C, Stoyanov S, Bojinova A, Rusev S. Dip coating apparatus for deposition of TiO$_2$ films. Ann Univ Sofia Fac Chim. 2006;**98–99**:73–82.

[30] Mitsuishi M, Kikuchi S, Miyashita T, Amao Y. Characterization of an ultrathin polymer optode and its application to temperature sensors based on luminescent europium complexes. J Mater Chem. 2003;**13**:2875–2879.

[31] Tyona MD. A theoretical study on spin coating technique. Adv Mater Res. 2013;**2**:195–208. doi: 10.12989/amr.2013.2.4.195

[32] Brinker CJ, Scherer GW, editors. Sol–gel Science, the Physics and Chemistry of Sol–Gel Processing. Boston: Academic Press; 1990.

[33] Hall DB, Underhill P, Torkelson JM. Spin coating of thin and ultrathin polymer films. Polym Eng Sci. 1998;**38**:2039. doi:10.1002/pen.10373

[34] Chen BT. Investigation of the solvent-evaporation effect on spin coating of thin films. Polym Eng Sci. 1983;**23**:399–403. doi:10.1002/pen.760230706

[35] Znaidi L, Illia GJAAS, Benyahi S, Sanchez C, Kanaev AV. Oriented ZnO thin films synthesis by sol–gel process for laser application. Thin Solid Films. 2003;**428**:257–262. DOI: 10.1016/S0040-6090(02)01219-1

[36] Scriven LE. Physics and applications of dip coating and spin coating. MRS Proc. 1988;**121**:717 DOI: 10.1557/PROC-121-71

[37] Chang YJ, Lee DH, Herman GS, Chang CH. High-performance spin-coated zinc tin oxide thin-film transistors. Electrochem Solid State Lett. 2007;**10**:H135–H138. doi:10.1149/1.2666588

[38] Amanuma K, Hase T, Miyasaka Y. Preparation and ferroelectric properties of SrBi2Ta2O9 thin films. Appl Phys Lett. 1995;**66**:221. DOI: 10.1063/1.113140

[39] Chung W, Sakai G, Shimanoe K, Miura N, Lee D, Yamazoe N. Preparation of indium oxide thin film by spin-coating method and its gas-sensing properties. Sens Actuat B: Chem. 1998;**46**:139–145. DOI: 10.1016/S0925-4005(98)00100-2

[40] Souza FL, Lopes KP, Nascente PAP, Leite ER. Nanostructured hematite thin films produced by spin-coating deposition solution: Application in water splitting. Solar Energy Mater Solar Cells. 2009;**93**:362–368. DOI: 10.1016/j.solmat.2008.11.049

[41] Natsume Y, Sakata H. Zinc oxide films prepared by sol-gel spin-coating. Thin Solid Films. 2000;**372**:30–36. DOI: 10.1016/S0040-6090(00)01056-7

[42] Ilican S, Caglar Y, Caglar M. Preparation and characterization of ZnO thin films deposited by sol-gel spin coating method. JOAM. 2008;**10**:2578–2583.

[43] Habibi MH, Sardashti MK. Structure and morphology of nanostructured zinc oxide thin films prepared by dip-vs. spin-coating methods. J Iran Chem Soc. 2008;**5**:603–609.

[44] Srinivasan G, Gopalakrishnan N, Yud Y, Kesavamoorthy R, Kumar J. Influence of post-deposition annealing on the structural and optical properties of ZnO thin films prepared

by sol–gel and spin-coating method. Superlattices Microstruct. 2008;**43**:112–119. DOI: 10.1016/j.spmi.2007.07.032

[45] Wang MC, Lin H, Yang TS. Characteristics and optical properties of iron ion (Fe3+)-doped titanium oxide thin films prepared by a sol–gel spin coating. J Alloys Compd. 2009; **473**:394–400. DOI: 10.1016/j.jallcom.2008.05.105

[46] Chen K, Lu Z, Ai N, Huang X, Zhang Y, Xin X, Zhu R, Su W. Development of yttria-stabilized zirconia thin films via slurry spin coating for intermediate-to-low temperature solid oxide fuel cells. J Power Sources. 2006;**160**:436–438. DOI: 10.1016/j.jpowsour.2006.01.079

[47] Nishiyama N, Tanaka S, Egashira Y, Oku Y, Ueyama K. Enhancement of structural stability of mesoporous silica thin films prepared by spin-coating. Chem Mater. 2002;**14**:4229–4234. doi:10.1021/cm0201246

[48] Messing GL, Zhang SC, Jayanthi GV. Ceramic powder synthesis by spray pyrolysis. J Am Ceram Soc. 1993;**76**:2707–2726. doi:10.1111/j.1151-2916.1993.tb04007.x

[49] Senthilnathan V, Ganesan S. Novel spray pyrolysis for dye-sensitized solar cell. J Renew Sust Energy. 2010;**2**:063102. doi:10.1063/1.3517228

[50] Milanova M, Koleva I, Todorovska R, Zaharieva J, Kostadinov M, Todorovsky D. Polymetallic citric complexes as precursors for spray-pyrolysis deposition of thin ferrite films. Appl Surf Sci. 2011:**257**:7821–7826.

[51] Milanova M, Zaharieva J, Todorovska R, Todorovsky D. Polymetallic citric complexes as precursors for spray-pyrolysis deposition of thin LaFeO3 films. Thin Solid Films. 2014;**562**:43–48.

[52] Uzunova-Bujnova M, Kralchevska R, Milanova M, Todorovska R, Hristov D, Todorovsky D. Crystal structure, morphology and photocatalytic activity of modified TiO2 and of spray-deposited TiO$_2$ films. Catal Today. 2010;**151**:14–20.

[53] Uzunova-Bujnova M, Todorovska R, Milanova M, Kralchevska R, Todorovsky D. On the spray-drying deposition of TiO$_2$ photocatalytic films. Appl Surf Sci. 2009;**256**:830–837.

[54] Todorovska R, Uzunova-Bujnova M, Milanova M, Todorovsky D. Spray-deposited TiO2 films for phenol destruction in water. Ann de l'Univ de Sofia "St. Kliment Ohridski", Faculte de Chimie. 2011:102/103:129–143.

[55] Nakaruk A, Reece PJ, Ragazzon D, Sorrell CC. TiO$_2$ films prepared by ultrasonic spray pyrolysis. Mater Sci Technol. 2010;**26**:469–472.

[56] Petrova N, Todorovska R, Milanova M, Todorovsky D. Spray-pyrolysis deposition of cerium-doped yttrium-iron garnet thin films. Asian Chem Lett. 2010;**14**:41–46.

[57] Perednis D, Wilhelm O, Pratsinis SE, Gauckler LJ. Morphology and deposition of thin yttria-stabilized zirconia films using spray pyrolysis. Thin Solid Films. 2005;**474**:84–95.

[58] Wilhelm O, Pratsinis SE, Perednis D, Gauckler LJ. Electrospray and pressurized spray deposition of yttria-stabilized zirconia films. Thin Solid Films. 2005;**479**:121–129.

[59] Akl Alaa A. Optical properties of crystalline and non-crystalline iron oxide thin films deposited by spray pyrolysis. Appl Surf Sci. 2004;**233**:307–319. DOI:10.1016/j.apsusc.2004.03.263

[60] Garcıa-Lobato MA, Hernandez VA, Garcıa HMH, Martınez AI, Pech-Canul MI. Fe2O3 thin films prepared by ultrasonic spray pyrolysis. Mater Sci Forum. 2010;**644**:105–108.

[61] Krunks M, Dedova T, Açik IO. Spray pyrolysis deposition of zinc oxide nanostructured layers. Thin Solid Films. 2006;**515**:1157–1160.

[62] Prasada Rao T, Santhoshkumar MC. Effect of thickness on structural, optical and electrical properties of nanostructured ZnO thin films by spray pyrolysis. Appl Surf Sci. 2009;**255**:4579–4584. doi:10.1016/j.apsusc.2008.11.079

[63] Martos M, Morales J, Sánchez L, Ayouchi R, Leinen D, F Martin, Barrado JRR. Electrochemical properties of lead oxide films obtained by spray pyrolysis as negative electrodes for lithium secondary batteries. Electrochim Acta. 2001;**46**:2939–2948. DOI:10.1016/S0013-4686(01)00512-6

[64] Kim SH, Liu BYH, Zachariah MR. Synthesis of nanoporous metal oxide particles by a new inorganic matrix spray pyrolysis method. Chem. Mater. 2002;**14**:2889–2899. doi:10.1021/cm010957g

[65] Medina DY, Orozco S, Hernandez I, Hernandez RT, Falcony C. Characterization of europium doped lanthanum oxide films prepared by spray pyrolysis. J Non-Crystal Solids. 2011;**357**:3740–3743. DOI: 10.1016/j.jnoncrysol.2011.07.021

[66] Chung W, Hong JY, Sun HP, Chun BH, Kim J, Sung HK. Spray pyrolysis synthesis of MAl2O4:Eu2+ (M = Ba, Sr) phosphor for UV LED excitation . J Cryst Growth. 2011;**326**:73–76. DOI: 10.1016/j.jcrysgro.2011.01.055

[67] Nakaruk A, Sorrell CC. Conceptual model for spray pyrolysis mechanism: fabrication and annealing of titania thin films. J Coat Technol Res. 2010;**7**: 665–676. doi:10.1007/s11998-010-9245-6

[68] Todorovsky DS, Todorovska RV, Milanova MM, Kovacheva D. Deposition and characterization of La2Ti2O7 thin films via spray pyrolysis process. Appl Surf Sci. 2007;**253**:4560–4565. DOI: 10.1016/j.apsusc.2006.10.016

[69] Todorovska, R V, Groudeva-Zotova S, Todorovsky DS. Spray pyrolysis deposition of α-Fe$_2$O$_3$ thin films using iron (III) citric complexes. Mat. Lett. 2002; **56**: 770-774. DOI: 10.1016/S0167-577X(02)00611-0

[70] Todorovska R, Petrova N, Todorovsky D. Spray-pyrolysis deposition of Y2O3 thin films using citric complexes as a starting material, Comptes Rendus de l'Academie Bulgare des Sciences. 2003;**56**:41–44.